

## Supplemental figure legends

### Figure S1: Changes in H3K9me2 and H3K27me3 associated with cardiac hypertrophy.

**A** (*left*) fibrosis as assessed by Masson's trichrome staining (n=6,5,6,5). (*middle*) qRT-PCR showing relative expression of *Col1a1* (n=5,5,4,7). (*right*) Cardiac contractility as assessed by the maximal velocity of the left ventricular (LV) wall (n=6,7,8,8). **B** Representative images of left ventricular sections following Masson's trichrome staining, which highlights areas of fibrosis in dark blue (scale bar, 50µm). **C** Segmentation of H3K9me2 or H3K27me3 levels in homogeneous LOCKs and BLOCs across a 10 megabase segment of chromosome 15. **D** Correspondence of ChIP-qPCR and ChIP-seq in PCM1+ nuclei. Bars indicate mean  $\pm$  s.e.m. fold enrichment over input for seq, over 20% of the input for K9me2 qPCR and over 4% of the input for H3K27me3. **E** Size distribution of regions homogeneously marked by H3K9me2 (LOCKs) and H3K27me3 (BLOCs) as determined by circular binary segmentation. Note that the Y-axis is trimmed to 250 to highlight differences in larger regions; original values are indicated in trimmed bars. Scatter plots of flow cytometric analyses of nuclei stained for PCM1. **F** Immunoblot analysis of H3K9me2 levels relative to total H3, in sorted, PCM1-positive nuclei extracted from sham-operated and aortic banded hearts. **G** Confocal images following immunofluorescence staining of WGA (red) and PCM1 (white) (*upper*) and H3K9me2 (green) (*lower*) in the left ventricular myocardium (scale bar, 50 µm). Nuclei are counterstained with DAPI. **H, I** (*left*) Jitter plots of H3K27me3 signal in PCM1+ nuclei, as detected upon immunofluorescence analysis of the left ventricular myocardium from aortic banded and sham-operated animals (*H*, n=4), and from exercised and control animals (*I*, n=3 and 4 respectively). *P*-values were calculated using nested ANOVA. (*right*) Representative confocal images of left ventricular myocardium following immunofluorescence staining of PCM1 (white) (*upper*) and H3K9me2 (green) (*lower*) in the left ventricular myocardium (scale bar, 50 µm). Nuclei are counterstained with DAPI. **J** ChIP-qPCR validation of changes in H3K9me2 upon aortic banding. Displayed are results from 2 unaltered loci (near *Ctnna3* and *Olr541*), and 3 loci displaying loss of H3K9me2 (*Nppa*, *Nppb* and *Myh7*). Bars represent means  $\pm$  s.e.m. of 5 independent experiments. **K, L** ChIP-seq quantification (reads per million and per kb, RPKM) of H3K9me2 levels at segments of chromosome 5 (*K*) and 15 (*L*) in PCM1+ nuclei sorted from hearts from postnatal day 1 (P1) and 3-month old (adult) rats. Lower panels: fold change in H3K9me2 levels when comparing hearts from P1 rats to postnatal day 3 rats, postnatal day 10 rats and adult rats. n=2. Chromosome coordinates are annotated in Mb. n=5 (D, J) or 4 (F) biological replicates; \*\*\**P*<0.001, \*\**P*<0.01, \**P*<0.05 by t-test (A, F and J) or nested ANOVA (H, I).

### Figure S2: Strand-specific sequencing of nuclear RNA from sorted CMs and correlation with H3K9me2 and H3K27me3 levels.

**A** Overlap of protein coding genes expressed in the unsorted input tissue and in nuclei sorted from the left ventricular wall of an adult rat's heart. **B** Distribution of reads over different annotated transcript species in the unsorted input and in sorted nuclei. An asterisk (\*) denotes that this sample was rRNA depleted prior to sequencing and this fraction therefore does not reflect the natural situation. **C** Correlation between read counts per gene in introns (*left*) and exons (*right*) in the unsorted input and in sorted nuclei. **D** RT-qPCR of differentially expressed transcript (*Tnnt2*, *Tnni3*, *Vim* and *Vwf*), in PCM1- and PCM1+ nuclei (n=4). **E** MA plot illustrating expression of protein coding genes in PCM1+ and PCM1- nuclei. Genes are colour-coded according to the q-value of their differential expression. **F** RNA-seq read alignments at the *Myh6* and *Gsn* loci in unsorted input, sorted nuclei, PCM1- nuclei and PCM1+ nuclei. **G** Ontology term enrichment of genes overexpressed in PCM1+ and PCM1- nuclei. *P*-value of enrichment is indicated by the colour in the box before each bar. **H, I** Density plots illustrating the genome-wide relation between RNA expression and H3K9me2 (*H*) or H3K27me3 (*I*). Data are quantified per bin of 10kb, and represented as log<sub>2</sub>((fragments + 1) per million). **J, K** Distribution of input-

normalized H3K9me2 (J) and H3K27me3 (K) levels ( $\log_2$ ) across centiles of the body of a metagene. Average values are displayed stratified per gene expression level ( $\log_2$  of read number per million and per kb) rounded to the nearest integer and colour-coded as in the legend below each plot. **L** Differentially expressed (DE) genes, ranked and colour-coded according their CM- or non-CM-specificity. DE genes that are among the top 10% most CM-specific are coloured green, the top 10% most non-CM-specific black, and deciles in between both shaded from green to black. Depicted are datasets generated by RNAseq from sorted rat CM nuclei in the current study (“sorted”), from mouse CMs sorted by gradient centrifugation by Papait *et al.* (Papait *et al.*, 2013) and from mouse whole tissue by Song *et al.* (Song *et al.*, 2012), and by expression microarrays from rat whole tissue by Strøm *et al.* (Strom *et al.*, 2005; Strom *et al.*, 2004) All gene sets were limited to those having a one-to-one orthologue between mouse and rat. **M** Correlation between AB-induced changes in gene expression and in H3K9me2. Differentially expressed and H3K9 dimethylated genes are highlighted in red. All other genes are in greyscales, pseudocoloured according to overplotting. The number of genes is indicated for each quadrant. n=2 (A-C, E-G) or 4 (H-K, M).

**Figure S3: Changes in H3K9me2 at the nuclear periphery and through H3K9 demethylases.**

**A** (*left*) Ratio of H3K9me2 signal at the nuclear periphery versus signal at the center of nuclei, and (*right*) representative images of H3K9me2 signal in PCM1+ nuclei (arrowed) from sham-operated and banded rat hearts (n=4 and 6 respectively). Signal intensities are pseudo-coloured as per the colour scale. **B** Protein levels of Ehmt2 relative to histone H3 in CMs sorted from rat hearts subjected to a sham or aortic banding operation 6 week prior. **C** Relative expression of H3K9me2 methyltransferases in CMs sorted from rat hearts subjected to a sham or aortic banding operation 6 week prior. **D** Relative expression of H3K9me3 demethylases (*Kdm4a* and *Kdm4b*) and H3K9me2 demethylases (*Kdm3a*, *Kdm3b* and *Kdm4c*), in CMs sorted from hearts hypertrophied because of aortic banding or training. Displayed in B-D are means  $\pm$  s.e.m of 3 (B) or 5 (C-D) independent measurements. \*\* $P < 0.01$ , \* $P < 0.05$  by t-test.

**Figure S4: Decreasing Ehmt2 activity causes pathological hypertrophy *in vitro*, in primary neonatal SD rat ventricular myocytes.**

**A** *Ehmt1* and *Ehmt2* expression in NRVMs upon exposure to A-366 and/or ET-1. **B** *Ehmt2* (n=3) and H3K9me2 (n=4) levels determined by immunoblotting in NRVMs treated with ET-1. **C** H3K9me2 levels, determined by immunostaining analysis of NRVMs upon exposure to A-366 treatment (n=5; *top*) or by immunoblot analysis (n=4; *bottom*). The immunostaining images presented are NRVMs also shown in Figure 4C, but stained here with antibodies against H3K9me2. **D** MTT cell viability assay of NRVMs incubated for 2 days with DMSO or A366. **E** RT-qPCR showing relative expression of *Nppa*, *Nppb*, *Myh6*, *Myh7*, *Ehmt1* and *Ehmt2* in NRVMs stimulated with insulin-like growth factor 1 (IGF1) relative to vehicle only. **F, G** Protein synthesis (F) and RT-qPCR for *Nppa*, *Nppb*, *Myh6* and *Myh7* (G) in primary NRVMs exposed to endothelin 1 (ET-1) or vehicle (water), and in response to G9a/GLP inhibition (UNC0638). **H** Immunoblot analysis of lysates prepared from NRVMs transfected with empty virus or virus encoding G9a-flag, using anti-flag and anti-Calnexin (Cnx) antibodies. Show is one representative experiment of 2 repeats. **I** Quantification (*left*) and representative immunoblot analysis (*right*) of lysates prepared from ET-1 or control-treated NRVMs transfected with empty virus or virus encoding G9a-flag, using anti-H3K9me2 and anti-H3 antibodies. Bars represent means  $\pm$  s.e.m. of 5 (panels A, D-G) or 3 (panel I) biological replicates. \*\*\* $P < 0.001$ , \*\* $P < 0.01$ , \* $P < 0.05$  by t-test (A, B, E-G, I).

**Figure S5: Hypertrophy of the left ventricle of sham and aortic banding (AB) operated mice, after perfusion with A-366 or after genetic Ehmt inactivation.**

**A** RT-qPCR showing relative expression of *Ehmt2* mRNA expression in sorted, PCM1+ nuclei from hearts of *Ehmt2<sup>fl/fl</sup>* versus *Ehmt2<sup>fl/fl</sup>;Tg(Myh6-MCM)* mice, 2 weeks after tamoxifen injection. Bars represent the mean  $\pm$  s.e.m. of 5 biological replicates. **B, C** Expression of G9a (**B**) and GLP (**C**) (encoded by *Ehmt2* and *Ehmt1* respectively) as assessed by immunofluorescence in respectively Nesprin+ nuclei of left ventricular tissue sections (scale bar, 20 $\mu$ m; n=5). **D-F** Representative images of the induction of hypertrophy as assessed by echocardiography (**D, E**; horizontal scale: 0.1 s; vertical scale: 2 mm) or MRI (**F**), in hearts subjected to A-366-mediated *Ehmt* inactivation (**D**) or genetic *Ehmt2* inactivation (**E, F**), with or without aortic banding (AB). Images were taken 10 days (**D**) or 14 days (**E, F**) after the aortic banding or sham operation. **G** Left ventricular weight relative to the body weight (**G**) in 4, 4, 5 and 5 mice of the indicated genotypes, 2 weeks after injection with tamoxifen or carrier (peanut oil). **H-J** Cardiac geometry (**H**), diastolic blood pressure (**I**) and systolic blood pressure (**J**) of mice of the indicated genotypes, 0, 1 or 2 weeks after injection with tamoxifen or carrier (n=5). **K** RT-qPCR showing relative expression of *Nppa*, *Nppb*, *Myh6*, *Myh7* and *Col1a1* in left ventricular tissue samples of mice of the indicated genotypes, 2 weeks after injection with tamoxifen or carrier. **L** RT-qPCR showing relative expression of hypertrophic marker genes *Nppa*, *Nppb*, *Col1a1*, *Myh6* and *Myh7* in left ventricular tissue samples 10 days after of aortic banding and/or A-366 perfusion. **M** log<sub>2</sub> expression of genes induced in rat cardiomyocytes by AB but not exercise (*left*), and in *Ehmt2<sup>fl/fl</sup>;Tg(Myh6-MCM)* hearts 2 weeks after tamoxifen injection (KO), or after AB (*mid left*). For comparison, the expression of these genes in embryonic stem (ES) cells as they differentiate to cardiomyocytes (CM) is also displayed (Wamstad et al., 2012) along with their expression in the heart of newborn mice (0w), 3 day-old, 10 day-old and 9 week-old mice (9w; *mid right*) (O'Meara et al., 2015). (*right*) changes in H3K9me2 occupancy (log<sub>2</sub>) in the LOCKs encompassing these genes, upon AB relative to sham. Colour codes are displayed on the far right, ranging from red to blue for relative expression changes (< -1.5 to >1.5), and from green to black for relative H3K9me2 occupancy changes (< -0.5 to > 0.5) (n=4). **N** RT-qPCR showing relative expression of *Ehmt1* and *Ehmt2* in left ventricular tissue samples 10 days after of aortic banding and/or A-366 perfusion. Bars represent means  $\pm$  s.e.m. of 5 (A, G-L, N) biological replicates. **O** Velocity over the aorta, banded 1 day prior, for wild-type mice implanted with minipumps delivering carrier or A-366 (*left*), and for *Ehmt2<sup>fl/fl</sup>* versus *Ehmt2<sup>fl/fl</sup>;Tg(Myh6-MCM)* mice (n=10,4,10,11 respectively). A vertical dashed line indicates experiments to inactivate *Ehmt* by chemical or genetic means conducted separately. Bars in panels A, K, L and N represent means  $\pm$  s.e.m. of 5 biological replicates. \*\*\*P<0.001, \*\*P<0.01, \*P<0.05, #P>0.4 by t-test (A, K, L and N) or nested ANOVA (B, C).

**Figure S6: Increased Mir217 upon pathological hypertrophy downregulates Ehmt expression in vitro.**

**A, B** Nascent *Ehmt* transcript levels in rat cardiomyocyte nuclei sorted from sham-operated and aortic banded (AB) hearts (**A**), and in neonatal rat ventricular myocytes (NRVMs) treated with endothelin 1 (ET-1) or water (**B**). **C** Alignment of Mir217 to predicted binding sites in the 3' untranslated region (UTR) of *Ehmts* across species. The Mir217 sequence is fully conserved between rodents and humans. Murine Watson-Crick base pairs are denoted using |; wobble base pairs using :. Bases showing positive pairing are highlighted in green. Alignment of the target site blockers for mir217 binding to rat *Ehmts* is shown below. **D** Activity of luciferase reporters constructs harbouring the 3'UTRs of *Ehmt1* and *Ehmt2* in HEK293 cells, upon transfection with mimics of microRNAs predicted to target the *Ehmt* 3'UTRs. Predictions were based on miRBase, PicTar and miRanda. Apart from *Mir217* mimics, only *Mir1b* mimics affected the luciferase activities. In line with earlier reports, *Mir1b* was however downregulated upon pathological hypertrophy and thus incompatible with a decreased *Ehmt* expression (not shown).

**E** Expression of hypertrophy markers *Nppa*, *Nppb*, *Myh6* and *Myh7* in NRVMs by RT-qPCR, in response to ET-1 and/or transfection of Mir217 mimics. **F** NRVM expression of *Ehmt1* and *Ehmt2* in NRVMs, in response to ET-1 with or without transfection of Mir217 antagonists. **G-J** Expression in NRVMs of mir217 (G), of native and mature *Ehmt1* (H) and *Ehmt2* (I) RNA, and of hypertrophy markers *Nppa*, *Nppb*, *Myh6* and *Myh7*, in response to ET-1 or water (control) after transfection of scrambled or *Ehmt1*- or *Ehmt2*-specific target site blockers as shown in panel C. Bars in A, B and D-F, and in G-J represent the mean  $\pm$  s.e.m. of respectively 5 and 4 biological replicates. \*\*\* $P < 0.001$ , \*\* $P < 0.01$ , \* $P < 0.05$  by t-test.

**Figure S7: Blocking Mir217 overexpression upon pathological hypertrophy downregulates Ehmt expression in vivo.**

**A, B** Expression of *Ehmt2* (A;  $n=4,4,5,5$  per condition indicated) and H3K9me2 levels (B;  $n=4,3,5,5$  per condition indicated) as assessed by immunofluorescence in respectively PCM1+ nuclei of left ventricular tissue sections (scale bar, 20  $\mu\text{m}$ ), isolated from sham or aortic banded hearts of wild-type mice injected with scramble or Mir217 antagonists. **C** Velocity over the aorta, banded 1 day prior, for wild-type mice injected with scramble or Mir217 antagonists ( $n=8$  or 5 respectively). \*\*\* $P < 0.001$ , \*\* $P < 0.01$ , \* $P < 0.05$  by nested ANOVA.

**Figure S8: Conservation of the MIR217-EHMT-H3K9me2 axis in humans.**

**A** Characteristics of hearts from 10 deceased male included in this study. Depicted are cardiac status, age in years, body mass index (BMI) and cause of death. **B, C** Nascent (B) and mature (C) transcript levels of *EHMT1* and *EHMT2* in HEK293 cells transfected with mir217 mimics. **D** *EHMT2* and H3K9me2 levels in HEK293 cells transfected with mir217 mimics, as assessed using immunoblotting. Bars represent the mean  $\pm$  s.e.m. of 5 (B, C) or 4 (D) biological replicates. \* $P < 0.05$  by t-test.

## **SUPPLEMENTAL EXPERIMENTAL PROCEDURES**

### ***MATERIALS***

All materials were molecular biology grade, and obtained from Sigma Aldrich (Dorset, UK), unless stated otherwise.

### ***ANIMALS AND PROCEDURES***

All experiments in the UK involving animals were performed in accordance with the guidelines from the code of practice for humane killing under Schedule 1 of the Animals (Scientific Procedures) Act 1986 (UK). All *in vivo* experiments were conducted in Norway in accordance with “Regulations on Animal Experimentation” under The Norwegian Animal Welfare Act and approved by the Norwegian Animal Research Authority (FDU application 3301, 3820 and 5338).

### ***CARDIAC HYPERTROPHY INDUCED BY BANDING OF THE ASCENDING AORTA IN RATS***

Male Sprague Dawley rats of ~170 g (6-7 week old; Taconic, Köln, Germany) were anesthetized and ventilated through endotracheal intubation with a mixture of 69% N<sub>2</sub>O, 29% O<sub>2</sub> and 2% isoflurane. A silk suture 3-0 was tightened around the ascending aorta proximal to the brachiocephalic trunk. Sham-operated animals served as controls and underwent the same surgical procedure, except tightening the silk suture around the ascending aorta. Buprenorphine was given as postoperative analgesia. After 6 weeks, only those rats were retained, that had non-failing hearts with detectable hypertrophy, defined as increased posterior wall thickness in diastole (>1.9 mm), increased left ventricular weight (>0.75 g) and preserved lung weight (<2.0 g).

### ***CARDIAC HYPERTROPHY INDUCED BY EXERCISE IN RATS***

Male Sprague Dawley rats of ~280 g (7-8 week old; Taconic) were assigned to interval training on a treadmill (Columbus Instruments, OH, US) with 25 degree inclination, with 5 days of acclimatization with running velocity for 6 m/min for 30, 45, 60, 75, 90 and 120 mins. Thereafter interval training was performed 6 days a week with 12 x 8 min intervals with 2 min resting period (6 m/min) after a warm-up period at 10 m/min. Exercise training was performed over six weeks at a running speed of 15 m/min increasing with 2 m/min each week. Rats not able to fulfill the exercise protocol were withdrawn from the study.

### ***A-366 IN VIVO EXPERIMENTS IN MICE***

C57BL/6j mice (15-18 g; 8-9 week old males; Taconic) were anesthetized and ventilated through endotracheal intubation with a mixture of 69% N<sub>2</sub>O, 29% O<sub>2</sub> and 2% isoflurane. Right thoracotomy was performed in the 2nd intercostal space, and the ascending aorta was ligated with a silk suture 8-0. Sham operated animals underwent the same procedure except suture placement. Only AB mice with a mild degree of stenosis (2.5-3.5 m/s in maximal flow velocity over aortic stenosis measured on the 2<sup>nd</sup> postoperative day) and no signs of congestion (LAD<2.0 mm) were included in the study. Mice were stratified by stenosis and then randomized to a 10 day treatment with either 30 mg/kg/day A-366 dissolved in 98:2 PEG 400:Polysorbate 80 or control treatment with 98:2 PEG 400:Polysorbate 80 without active compound administered by subcutaneous delivery through miniosmotic pumps (Alzet, CA, US).

### ***CARDIOMYOCYTE-SPECIFIC G9A KNOCK-OUT***

C57BL/6j *Ehmt2*<sup>fl/fl</sup> mice (Tachibana et al., 2007) were crossed with cardiomyocyte-restricted (*Myh6* promoter) tamoxifen-inducible MerCreMer expressing transgenic mice (backcrossed into C57BL/6j, Taconic for >10 generations) (Sohal et al., 2001) to generate C57BL/6j *Ehmt2*<sup>fl/fl</sup>;Tg(*Myh6*-MCM) mice. Littermate *Ehmt2*<sup>fl/fl</sup> mice were used as controls. Genotyping of *Ehmt2*<sup>fl/fl</sup> and *Myh6*-MCM was performed as previously described (Andersson et al., 2009; Tachibana et al., 2007). Aortic banding and sham operations of 8-10 week old mice (males and females) were done as described for the A-366 experiments. Tamoxifen (40 mg/kg) was administered the first postoperative day by a single intraperitoneal injection, in order to avoid transient cardiomyopathy by repetitive tamoxifen administration (Hougen et al., 2010).

### ***MIR217 ANTAGOMIR EXPERIMENT IN MICE***

To test the *in vivo* effect of Mir217 upregulation, C57BL/6j mice (7 week old; Janvier, France) were subjected to treatment with antagomirs (Exiqon, Denmark). Mice were randomized to antagomir treatment or control based on echocardiographic examination 1d after surgery, and only mice with moderate stenosis (maximal blood velocity <3.5 m/s) and no atrial and ventricular dilatation was included in the study. Antagomir or control was injected in the jugular vein 1d and 4d after AB at 10 mg/kg from a 4 mg/mL PBS solution. MRI and echocardiographic evaluation of cardiac geometry and function was examined 14d after AB, before LV samples were harvested in deep surgical anesthesia for later molecular analysis.

### ***ECHOCARDIOGRAPHY, MAGNETIC RESONANCE IMAGING AND CARDIAC PHENOTYPING***

For echocardiography, the Vevo2100 system (VisualSonics Inc, Canada) was used to obtain long and short axis images of the left ventricle and left atrium, Doppler signals in the mitral, pulmonary and aortic valves and tissue velocity in the left ventricular posterior wall.

MRI was performed on a 9.4T preclinical MR system (Agilent Technologies, Inc., CA) with high-performance gradient (60 mm ID, rise time 180  $\mu$ s, max strength 100 gauss/cm) and a quadrature volume RF coils (35 mm ID, Rapid Biomedical, Washington, USA) dedicated to mouse imaging. Anesthesia was induced in an anesthesia chamber with a mixture of 96% O<sub>2</sub> and 4% isoflurane, and further maintained by administration of a mixture of O<sub>2</sub> and 1.0-1.5% isoflurane through mask ventilation. Heart rate, body temperature and respiration rate were constantly monitored during experiments. Animal temperature was maintained by heated air. MRI cine data sets were acquired using a motion compensated gradient echo sequence. Left ventricular short-axis slices (8-10) were acquired, covering the heart from base to apex. Central imaging parameters: echo-/repetition time=2.1/4.6 ms; field-of-view =25.6x25.6 mm; acquisition matrix 128x128; slice thickness =1.0 mm; flip angle 15°; averages =2. MRI cine data were obtained with ECG-triggering and respiration gating. The total experiment duration was 40 min per animal. MRI data was analyzed using Fiji software with the operator blinded to animal groups (Schindelin et al., 2012). Mass estimates were obtained in diastole and systole, and <5% variance between mass calculation in diastole and systole was accepted.

After final echocardiography, animals were intubated and ventilated through endotracheal intubation while mice were ventilated by mask ventilation. The chest was opened, followed by excision of the heart. The four heart chambers were rapidly dissected, weighted and frozen in liquid nitrogen. Left ventricular myocardium was used for further molecular analysis.

### ***HUMAN HEART TISSUES***

Heart specimens were provided by the Department of Forensic Medicine in Stockholm, Sweden. Ethical permissions have been obtained from local ethical committees. The myocardial left ventricles were collected after receiving the informed consent of relatives and stored at -80°C until further use. PCM1+ nuclei were sorted as described (Bergmann et al., 2011; Bergmann et al., 2015).

### ***IN VITRO MODELS OF HYPERTROPHY***

Gravid time-mated Sprague-Dawley rats were obtained from Charles River. Ventricular myocytes from neonatal (P3) Sprague-Dawley rats (NRVMs) were isolated, seeded and cultured identically as described (Drawnel et al., 2012). NRVMs were seeded at a monolayer density, and were required to beat spontaneously throughout the experiment. 48 h after seeding, myocytes were washed into serum-free medium (DMEM/M199 4:1, 1 mM sodium pyruvate, 5.5  $\mu$ g/mL transferrin, 5 ng/mL Na<sub>2</sub>SeO<sub>3</sub>, 1 $\times$  Antibiotic-Antimycotic (Life Technologies), and 3  $\mu$ M cytosine  $\beta$ -d-arabinofuranoside) and serum-starved for 24 h. Cells were subsequently left unstimulated, stimulated with 100 nM endothelin-1 (ET-1) or with 10 nM insulin-like growth factor 1 (IGF-1) (both from Millipore), in the presence of UNC0638 (350 nM), A-366 (0.5  $\mu$ M) or its carrier (DMSO) for 48 h.

### ***ANALYSIS OF POST-TRANSCRIPTIONAL STABILITY OF EHMTS BY 3'UTR REGULATION***

Sequences corresponding to the 3'UTR of murine *Ehmt1* and *Ehmt2* were synthesized and cloned by Life Technologies into the pmirGLO Dual-Luciferase miRNA Target Expression Vector (Promega) to

generate pmirGLO-Ehmt1 or 2 -3'UTR plasmids. NRVMs or HEK293 cells, seeded in a 96-well tissue culture plate, were transfected with 200 ng of this plasmid using Lipofectamine 3000 (Life Technologies) according to manufacturer's instructions. 24 h later, either ET-1 (100 nM) or water were added, or 75 pmoles of Mir217 mimic and its scrambled control were transfected using Lipofectamine 3000. For antagomiR experiments, 3 pmoles of Mir217 or scrambled antagomir (Shanghai GenePharma) were transfected using Lipofectamine 3000, 24 h prior to ET-1 treatment. 24 h later, the activity of Renilla and firefly luciferases was assessed using the Dual-Luciferase® Reporter Assay System (Life Technologies), with luminescence measured on an EG & G Berthold MicroLumatPlus LB96V Microplate luminometer (Berthold Technologies, Vilvoorde, Belgium). Duplicate readings from three replicate wells were obtained per experiment, and the experiment was repeated 5 times. For RNA and protein expression analyses, quantities were proportionally scaled up to 12-well and 6-well formats respectively.

### ***ANALYSIS OF MICRORNA- MEDIATED TARGETING OF THE EHMT 3'UTR***

miRBase, PicTar and miRanda were used to scan for conserved microRNA binding sites, yielding 4 miRNAs for further analysis (Mir1b, Mir18a, Mir217 and Mir206). First, 200 ng of either of the pmirGLO-Ehmt-3'UTR plasmids was transfected using Lipofectamine 3000 (Life Technologies) into HEK293 or HeLa cells, seeded on a 96-well tissue culture plate. After 24 h, cells were transfected with 3 pmoles of microRNA mimic double stranded RNA oligonucleotides (Shanghai GenePharma, Shanghai, China). A scrambled sequence was used as negative control. Luminescence was measured after 24 h as described for NRVMs.

### ***THE EFFECT OF MIR217 MIMIC TRANSFECTION IN HEK293 CELLS***

HEK293 cells were seeded on 96-well or 6-well culture dishes at a density of  $3 \times 10^4$  and  $0.3 \times 10^6$  for RNA or protein respectively. 24 hours later, cells were transfected with 3 pmoles (96 well dish) or 75 pmoles of microRNA mimic double stranded RNA oligonucleotides or scrambled negative control oligonucleotide (Shanghai GenePharma, Shanghai, China) using Lipofectamine 3000 (Life Technologies, manufacturer's protocol omitting the P3000 reagent). 48 hours later, cells were harvested in TRIzol (Life Technologies) for RNA for RT-qPCR in 96 well dishes or in cold PBS in 6 well dishes for protein for immunoblots.

### ***OVEREXPRESSION OF G9A IN NRVMs***

Human *Ehmt2* cDNA in pCMX was obtained from Iannis Talianidis (Boulias and Talianidis, 2004). *Ehmt2* cDNA was isolated by restriction digest with EcoR1 and BamH1 and subcloned into respective sites in pdc515(io) (Microbix, Mississauga, Canada). Annealed oligonucleotides encoding a FLAG tag were inserted into an EcoR1 site at the 5' end of *Ehmt2* to generate an in frame fusion. For generation of virus, the Flag tagged *Ehmt2* was subcloned into pENTRY/D-TOPO following PCR amplification and subsequently transferred into the adenoviral cosmid pAD/CMV/V5 by Gateway cloning (AdMax, Life Technologies). Viral particles were generated following transfection of this cosmid into HEK293 cells using Lipofectamine 2000 (Life Technologies). Virus was amplified in HEK293 cells and purified by column using the Vivapure Adenopack 100 kit (Sartorius, Surrey, UK). Virus was titrated by end point dilution and an appropriate volume, required to induce >90% infection, was used. An empty virus was used as control. NRVMs were infected in media containing virus. After 8 h, cells were treated with ET-1 as previously described (Higazi et al., 2009) and incubated for a further 48 h prior to harvesting.

### ***NUCLEAR ISOLATION***

To minimize handling times and to control potential inter-experimental artefacts, nuclei were isolated and sorted from 2 left ventricular wall samples per experiment, one hypertrophic sample and one corresponding control sample. Methods for nuclear isolation were based on a previously described method (Bergmann et al., 2011). All buffers were precooled, supplemented with dithiothreitol (1  $\mu$ M), actinomycin D (1mg/L), *cOmplete* protease inhibitor (PI) cocktail (Roche; 0.5  $\mu$ L/mL) and SUPERase·In (Ambion; 200 U/mL), and buffered with 10 mM Tris-HCl to pH 8.0. Frozen hearts were thawed in 10 mL lysis buffer (0.32 M sucrose, 5 mM CaCl<sub>2</sub>, 5 mM EDTA, 0.5 mM EGTA, 3 mM Mg(CH<sub>3</sub>COO)<sub>2</sub>) and homogenized using an IKA ultra-Turrax (20,000 RPM, 15 sec). After addition of 30 mL lysis buffer, the homogenate was

dounced 10× on ice, filtered consecutively over mesh, a 100 µm and a 70 µm cell strainer and spun for 10 min (700×G; 4°C). The resulting pellet was dissolved in 10 mL centrifuge buffer (2.1 M sucrose, 3 mM Mg(CH<sub>3</sub>COO)<sub>2</sub>, and 5 mM EDTA), and superimposed upon 5 mL centrifuge buffer in an autoclaved Thinwall Ultra-Clear Tube (Beckman Coulter, High Wycombe, UK). Tubes were loaded in a precooled rotor (SW32.1Ti) and spun for 60 min (26,000×G; 4°C) in an OPTIMA MAX Ultracentrifuge (both from Beckman Coulter). The resulting pellet was dissolved in 1.5 mL sorting buffer (0.43 M sucrose, 70 mM KCl, 2 mM MgCl<sub>2</sub> and 5 mM EDTA) and labelled for 1 h on ice using 3 µL anti-PCMI antibody (HPA023374) that was pre-incubated for 15 min with 2 µL Alexa Fluor 488 Goat Anti-Rabbit IgG (H+L) Antibody (Life Technologies).

### ***FLOW SORTING***

Nuclei were sorted on an Influx streaming air high-speed cell sorter or Aria III (BD Biosciences, Oxford, UK) using a gating strategy as described (Bergmann et al., 2009). Post-sorting flow cytometric analyses were done using FlowJo (v9.6.3) and Bioconductor's flowCore package (Hahne et al., 2009). Nuclei were sorted into Protein LoBind tubes (Eppendorf, Stevenage, UK) on a cooled tube holder. Tubes were preloaded with either 50 µL EDTA (10 mM) and SUPERase-In (100 U), or 100 µL MgCl<sub>2</sub> (10 mM), CaCl<sub>2</sub> (50 mM) with 1.5 µL *cOmplete* PI cocktail and 200 µg bovine serum albumin (New England Biolabs, Hitchin, UK), respectively for nuclear RNA and chromatin extraction. For RNA extraction, 100,000 PCMI-positive nuclei were collected, whereas 0.3-1 million nuclei were sorted for chromatin extraction. For comparison of unsorted and sorted nuclei, the input samples corresponded to a 350 µL aliquot of the original homogenized sample, and the nuclear samples corresponded to 400,000 nuclei not gated for PCMI staining. The solution of sorted nuclei for RNA extraction was mixed with 3× its volume of TRIzol LS reagent (Life Technologies) and 2 µL glycogen (Life Technologies), and stored for at most one month at -80°C until further processing; nucleosome extraction was proceeded with immediately.

### ***NUCLEOSOME EXTRACTION, CHROMATIN IMMUNOPRECIPITATION, DNA PURIFICATION AND END REPAIR***

The solution of sorted nuclei for nucleosome extraction was topped up with MNase buffer (0.32 M sucrose, 4 mM MgCl<sub>2</sub>, 1 mM CaCl<sub>2</sub> and 1 µL/mL *cOmplete* PI cocktail) to a final volume of 1.5 mL and centrifuged for 10 min (1,000×G, 4°C). All but 100 µL supernatant was removed, and nuclei were gently suspended in an additional 1.4 mL MNase buffer and centrifuged for 10 min (1,000×G, 4°C). All but 100 µL supernatant was again removed, and the pelleted nuclei were suspended to a concentration of 4,000 nuclei (as counted by flow cytometry) per µL in MNase buffer. Micrococcal nuclease (Affymetrix USB, Staufien, Germany) was subsequently added (20 U/mL) to the nuclei suspension. In order to digest the chromatin to a predominantly mononucleosomal resolution, the reaction was stopped after 8 min of incubation at 37°C by transfer to ice and by the addition of ½ volume of nucleosome extraction buffer (15 mM EDTA, 0.3% Triton X-100, 10 mM Na<sub>2</sub>HPO<sub>4</sub>, 3.5 mM KH<sub>2</sub>PO<sub>4</sub>, 1.5 M NaCl, 20 µg/mL and 3 µL/mL *cOmplete* PI cocktail at pH 7.4). Nucleosomes were subsequently extracted at 4°C overnight on a vertical rotor (30 RPM). The next day, nuclear debris was removed by centrifugation for 10 min (21,000×G, 4°C), after which 10 µL Protein G Dynabeads (Life Technologies) were added to the supernatant for pre-clearing the solution and removing the remainder of the antibodies that were used for nuclei labelling. After 1 h at 4°C on a vertical rotor (30 RPM), the beads were removed by magnetic separation, and the solution split in 2 equal fractions. Per volume, 2.5 volumes of CHIP buffer (3 mM Na<sub>2</sub>HPO<sub>4</sub>, 1 mM KH<sub>2</sub>PO<sub>4</sub>, 50 mM NaCl, 5 mM EDTA, 2 µg/mL BSA and 1 µL/mL *cOmplete* PI cocktail at pH 7.4) were added, as well as per fraction either the mouse monoclonal anti-H3K9me2 (clone MABI 0307; Active Motif, La Hulpe, Belgium) or the rabbit polyclonal anti-H3K27me3 (07-449; Millipore, Watford, UK) antibody, each at 1 µg/mL. These solutions were kept overnight on a vertical rotor at 4 °C (5 RPM) to allow for antibody binding. On the next day, 20 µL Protein G Dynabeads were added to each solution, and after mixing on a vertical rotor at 4°C (5 RPM) for 2 h, beads were magnetically separated and the cleared solution transferred to a new tube to be kept as input fraction. Beads were washed 8 times with RIPA buffer (50 mM Tris-HCl, 1 mM EDTA, 1% NP-40, 0.7% sodium deoxycholate, 0.5 M LiCl and 1 µL/mL *cOmplete* PI cocktail at pH 7.5) and once with TE buffer (50 mM Tris-HCl, 1 mM EDTA and 1 µL/mL *cOmplete* PI cocktail at pH 7.5), after which beads were resuspended in 200 µL TE and transferred to a new tube. Proteinase K (2 mg) was subsequently added to each tube (including input fractions), and after incubation

at 42°C for 30 min, DNA was extracted using the QIAquick PCR purification kit (QIAGEN, Manchester, UK) as follows: binding buffer PB with pH indicator was added directly to the suspension, pH adjusted using Na(CH<sub>3</sub>COO) and after an incubation of 10 min (and magnetic separation of the beads from the ChIP samples), the DNA binding, washing and elution in 50 µL water was performed as per the kit's instructions. Purified DNA was rendered blunt ended using the NEBnext End Repair Module (New England Biolabs) as per the manufacturer's instructions.

### ***RNA EXTRACTION, FRAGMENTATION, CDNA AND SECOND STRAND SYNTHESIS***

RNA was extracted using TRIzol LS following the manufacturer's instructions, and dissolved in 20 µL TE buffer supplemented with 20U SUPERase-In. Total RNA from the input sample was depleted of ribosomal RNA using the RiboMinus Human/Mouse Transcriptome Isolation Kit (Life Technologies). Nuclear RNA was used in its entirety as extracted. Genomic DNA was removed from all RNA samples using the TURBO DNA-free kit (Life Technologies). RNA was subsequently reverse transcribed using SuperScript III Reverse Transcriptase (Life Technologies) as follows: 3 µg Random Primers (mostly hexamers; Life Technologies) were added to 10 µL RNA and 8 µL 5× First-Strand Buffer. This mixture was heated to 94 °C for 3 min for RNA fragmentation, and incubated on ice for at least 1 min. Next 2 µL dNTP Mix (10 mM) (Life Technologies) were added, as well as 4 µl DTT (100 mM), 40U SUPERase-In, 400U SuperScript™ III Reverse Transcriptase and 8 µg Actinomycin D. Water was added to make up the volume to 40 µL, and the sample was incubated at 25 °C for 5 min 50 °C for 30 min and inactivated at 70 °C for 15 min. cDNA-RNA duplexes were purified using 72 µL Agencourt AMPure XP (Beckman Coulter) and eluted in 20 µL of the following second-strand synthesis reaction mix: 0.33 mM dATP, dCTP and dGTP (Life Technologies), 0.33 mM dUTP (Sigma Aldrich), 0.25 U Ribonuclease H (Life Technologies) and 10 U DNA polymerase I (New England Biolabs). The reaction was allowed to proceed for 2.5 h at 16 °C.

### ***PREPARATION OF LIBRARIES AND HIGH-THROUGHPUT SEQUENCING***

End repair or second strand synthesis reactions were purified using Agencourt AMPure XP (Beckman Coulter) and eluted in 15 µL dA-tailing mix (NEBNext dA-Tailing Module; New England Biolabs). This mix was incubated at 37 °C for 30 min, purified using Agencourt AMPure XP (Beckman Coulter) and eluted in 14 µL of pre-annealed barcoded adapters at a 20× molar amount relative to the estimated amount of dA-tailed DNA. Next, 4 µL 5× Ligation Buffer and 2 µL Quick Ligase (NEBnext Quick Ligation Module; New England Biolabs) were added, and the reaction was incubated for 15 min at 37 °C. These reactions were again purified using Agencourt AMPure XP (Beckman Coulter) and eluted in 50 µL water for ChIP sequencing, or 49 µL TE buffer and 1 µL USER enzyme mix (New England Biolabs) for nuclear RNA sequencing. The latter mix was incubated at 37 °C for 30 min and at 95 °C for 5 min.

To amplify these libraries, 50 µL Phusion High-Fidelity PCR Master Mix with HF Buffer (Thermo Scientific, Loughborough, UK) was added to each sample, together with primer 1 and 2 oligonucleotides to a final concentration of 500 nM. Each reactions was distributed between 4 PCR tubes and PCR was performed in a thermal cycler using the following programme: initial denaturation at 98°C for 30 seconds, amplification over 18 cycles of 98 °C, 65 °C and 72 °C for respectively 10, 30 and 30 seconds, and a final extension at 72 °C for 7 min. PCR reactions were purified using the QIAquick PCR purification kit, eluted in 25 µL, mixed with 10 µL loading buffer (200 mg/mL Ficoll 400, 15 mg/mL Orange G and 2× Tris/Borate/EDTA buffer) and loaded on a 1.7% TBE agarose gel, prestained with SYBR safe DNA gel stain (Life Technologies). DNA was separated by electrophoresis at 4V/cm for 2 h at 4 °C, and 200 to 400 bp fragments were excised and purified using the QIAquick Gel Extraction Kit (QIAGEN) as per the manufacturer's instructions. DNA fragment size was verified on a 2100 Bioanalyzer Instrument using a High Sensitivity DNA Analysis Kit (both from Agilent Technologies Inc., Santa Clara, USA), and DNA concentration was verified using the Quant-iT PicoGreen dsDNA Assay Kit (Life Technologies). DNA libraries were sequenced on an Illumina HiSeq 1000 (Illumina, Essex, UK) using either the default RTA software, or a custom programme that consisted of annealing of Illumina Read 1 sequencing primer, 4 dark cycles, 46 light cycles, denaturation, annealing of Illumina Read 1 sequencing primer and 5 light cycles to read the indexing barcode. The latter modification was introduced because the low complexity of the first bases from the indexing barcode yielded incorrect cluster definitions and consequently lowered the number of high quality reads.

## ***RNA SEQUENCING: DATA ANALYSIS***

Annotations of functional genomic features and their coordinates were obtained from Ensembl (Release 69). All reads were aligned using Bowtie against the rat genome (build 3.4) using settings `-n 1 -m 1 --strata --best` (i.e. requiring at most one unique mapping per read, allowing one mismatch) (Langmead et al., 2009). Results were converted to the BAM file format using SAMtools (Li et al., 2009). Read counts of genomic features of interest were determined using the SeqMonk Mapped Sequence Data Analyser (Version 0.22.0; [www.bioinformatics.babraham.ac.uk/projects/seqmonk/](http://www.bioinformatics.babraham.ac.uk/projects/seqmonk/)), and further processed using R version 2.15.1 (Team, 2012).

All reads were aligned using Bowtie against the rat genome (build 3.4) using settings `-n 1 -m 1 --strata --best` (i.e. requiring at most one unique mapping per read, allowing one mismatch)<sup>27</sup>. Read counts of genomic features of interest were determined using the SeqMonk Mapped Sequence Data Analyser (Version 0.22.0; [www.bioinformatics.babraham.ac.uk/projects/seqmonk/](http://www.bioinformatics.babraham.ac.uk/projects/seqmonk/)), and further processed using R version 2.15.1<sup>28</sup>. Analysis of gene expression was based on strand-specific read counts, with only reads mapping to the strand opposite of the annotated gene orientation being counted. To assess issues related to strand-specificity of the RNA-seq, we assessed the fraction of all reads per gene mapping to the opposite strand. In the top 10% most strand-specific expressed genes, this fraction was on average 99.96%, indicating that at most ~0.04% of reads map to the annotated orientation for non-biological causes (e.g. technical or mapping issues). Differential RNA expression was assessed based on differences between each treatment and control sample, paired per sorting experiment, using a Chi-squared test. The median of the resulting *P* value per gene from 4 independent experiments was calculated, and corrected for multiple testing as described (Benjamini and Hochberg, 1995).

## ***CHIP SEQUENCING: DATA ANALYSIS***

ChIP-seq reads were extended *in silico* to 150 bp, for them to correspond to the average length of the mononucleosomal DNA fragments observed upon 2100 Bioanalyzer measurements. Read counts of genomic features of interest were determined using the SeqMonk Mapped Sequence Data Analyser (Version 0.22.0; [www.bioinformatics.babraham.ac.uk/projects/seqmonk/](http://www.bioinformatics.babraham.ac.uk/projects/seqmonk/)), and further processed using R version 2.15.1 (Team, 2012). Except for cluster analyses, histone methylation was always assessed in autosomal 10 kb windows, with a 10 kb step size. Windows with no or poor mapping (resp. gaps in the genome build or highly repetitive sequences) were not considered. Such windows were identified as having read counts that were over 6 times the third interquartile range different from the median input read counts. Read counts for input samples were highly concordant (average Pearson's  $r = 0.994$ ) and failed to show significant differences between H3K9me2 and H3K27me3, or between the different treatments (q-value exceeding 0.5 for all). All input samples were therefore binned and treated as one dataset in subsequent analyses. To identify regions of estimated equal H3K9me2 or H3K27me3 levels, circular binary segmentation was applied on the combined control datasets using the DNAcopy package using default parameters (Venkatraman and Olshen, 2007). Circular binary segmentation was applied using the *segment* function, using the hybrid approach for the computation of the *P*-value of the maximal *t*-statistic, requiring a significance level lower than 0.01 to accept change-points, and a minimum of 5 probes per segment (Venkatraman and Olshen, 2007). Differences in these segments between paired treated and control samples were assessed using a paired *t*-test on the 10kb window read counts. Counts were normalized in SeqMonk by adjusting them to have a matched distribution across all samples. Average histone methylation levels per segment were required to differ at least 20%, and to differ in at least 3 out of 4 paired treatment-control experiments in the same direction. Additionally, *P*-values from *t*-tests were corrected for multiple testing (Benjamini and Hochberg, 1995), and segments were only considered significantly different if q-values were below 0.1.

## ***GENE ONTOLOGY ANALYSES***

Functional enrichment was analyzed using gene ontology (GO) annotations. The topGO package was applied in R to decorrelate the inherently hierarchical GO graph structure, and thus to detect only the locally most significant terms for each dataset. Term selection was carried out using the combined weight and elimination algorithm (*weight01*) (Alexa and Rahnenfuhrer, 2010). Significance was calculated using Fisher's exact test and taken to be significant if below 0.05. Because these *P*-values were conditioned on

neighboring terms and therefore not independent, there was no possibility (or necessity) for multiple testing correction. When comparing GO term enrichments between datasets, the *classic* algorithm was used to score GO terms in topGO, and enrichment scores and *P*-values corresponding to terms appearing in either of the individual *weight01* term lists were extracted and reported.

### **GENE EXPRESSION ANALYSIS BY RT-QPCR**

NRVMs were plated in 24-well plates with biological duplicates for each treatment. RNA was extracted using the PureLink *Pro* 96 total RNA Purification Kit (Life Technologies) or by TRI-Reagent (Sigma), and 150 ng RNA was primed with 2 µg random hexamers (Roche) and reverse transcribed using SuperScript II (Life Technologies) following the manufacturer's instructions. cDNA was analyzed by real-time quantitative PCR for the expression of genes of interest on a CFX384 (Bio-Rad) using the Platinum SYBR Green qPCR SuperMix-UDG (Life Technologies) and oligonucleotide primers (sequence available upon request). Gene expression was normalized to the geometric mean of the expression of 3 housekeepers (*Sdha*, *B2m* and *Gapdh*) following the  $\Delta\Delta C_t$  method (Vandesompele et al., 2002), and expressed relative to unstimulated untreated samples.

### **PROTEIN SYNTHESIS ANALYSIS BY <sup>3</sup>H-LEUCINE INCORPORATION MEASUREMENTS**

NRVMs were plated in 24-well plates with biological duplicates for each treatment. At the time of agonist addition, 16.5 KBq [<sup>3</sup>H] leucine (PerkinElmer, Cambridge, UK; Specific activity 1.48-2.22 TBq (40-60 Ci)/mmol) was added per well. Media were refreshed after 24 h. After 48 h, cells were washed twice with PBS, incubated for 1 h on ice with 0.5 mL of a 5% (V/V) Trichloroacetic acid solution, washed once with cold PBS and incubated for 1 h with 0.5 mL 1 N NaOH on a flat bed shaker. Plate bottoms were subsequently scraped, and the solution was added to 5 mL scintillation liquid. Scintillation counts were recorded, averaged across duplicates and expressed relative to unstimulated untreated samples.

### **PERINUCLEAR ANF EXPRESSION ANALYSIS USING HIGH-THROUGHPUT IMMUNOFLUORESCENCE**

NRVMs were plated in 96-well plates with biological triplicates for each treatment. Following treatment, cells were washed 3 times with PBS, fixed for 15 min at room temperature using fixation buffer (2% Paraformaldehyde and 0.05% Glutaraldehyde in PBS), washed 3 times with PBS, permeabilized for 15 min using 0.2% Triton X-100 in PBS and blocked using blocking buffer (0.1% Triton X-100 and 5% normal goat serum [Jackson ImmunoResearch] in PBS) for 1 h. Thereafter, cells were incubated for 1 h with antibodies against ANF (SAB2501837, Sigma), H3K9me2 (ab1220, Abcam) and  $\alpha$ -actinin (A7732, Sigma-Aldrich) prepared at a dilution of 1:500 in blocking buffer, and washed 4 times for 15 min using 0.1% Triton X-100 in PBS. Secondary antibodies coupled to Alexa Fluor 488, 568 and 647 (Life Technologies) were added at a dilution of 1:500 in staining buffer (0.1% Triton X-100 and 2% normal goat serum in PBS) and incubated for 1 h. Finally, cells were washed 4 times for 15 min using 0.1% Triton X-100 in PBS, and nuclei were stained by incubation for 20 min with Hoechst (Life Technologies; 1 µg/ml in PBS).

Images were captured on a BD Pathway 855 (BD Biosciences) running on AttoVision software (BD Biosciences), using a 40× UPlan FLN air objective (Olympus) and an Orca ER camera (Hamamatsu Photonics). Nine tiled 3×3 images were acquired per well, and analysed using AttoVision. Areas of positive Hoechst staining were defined as nuclei (~800 nuclei imaged per well), and the perinuclear region was defined as 3 pixels inside and 6 pixels outside the nuclear border (~1500 pixels). Average pixel intensity in the perinuclear region was calculated for green and red signals (respectively  $\alpha$ -actinin and ANF). Non-myocyte cells were identified as lacking  $\alpha$ -actinin staining and were not analyzed (~5%).

### **IMMUNOFLUORESCENCE ANALYSIS OF HEART SECTIONS**

Snap-frozen mouse and rat heart samples were embedded in optimum cutting temperature compound (VWR), cryo-sections (thickness 10 µm) were collected on SUPERFROST PLUS microscope slides (VWR), fixed in 4% Paraformaldehyde in PBS for 15 min (or for 15 min in methanol for EHMT1 staining), permeabilised in 0.5% Triton-X100 in PBS for 1 hour at room temperature, and blocked in 5% Chemiblock (Millipore 2170) in PBS with 0.1% Triton-X100 (PBS-TX) for 1 h. Sections were subsequently incubated overnight at 4 °C in blocking buffer with primary antibodies against H3K9me2 (Abcam ab1220, 1:500),

EHMT2/G9a (Cell Signalling, 3306, C6H3 11:00), H3K27me3 (Millipore 07-449, 1:500), EHMT1/GLP (ab135484 or ab41969), Nesprin (Glenn E. Morris 7A12, 1:100) and PCM1 (Sigma HPA023374, 1:500). Samples were washed extensively in PBS-TX, and incubated with Alexa Fluor 568 Goat Anti-Rabbit (Invitrogen A-11036) and Alexa Fluor 488 Goat Anti-Mouse (Invitrogen A-11029) secondary antibodies (both at 1:500 in PBS-TX) for 1 h at room temperature. Where required, an Alexa Fluor 647 conjugate of wheat germ agglutinin (Invitrogen) and DAPI were included to identify the glycoproteins enveloping myocytes and the DNA in nuclei, respectively. Sections were mounted in Vectashield with DAPI (Vector Labs) and imaged on a Nikon A1R confocal microscope through a Plan Fluor DIC H N 40x oil objective (N.A.=1.3). Image stacks were collected over a 2  $\mu\text{m}$  stack thickness (0.2  $\mu\text{m}$  z-step). Sections from multiple hearts were cut and labeled with antibodies, and all imaged with identical image capture settings on the same day. Data presented are background-subtracted grey levels, and no data normalization was performed.

Frozen human cardiac tissue from the left ventricle was prepared through the CryoJane Tape-Transfer System. 14  $\mu\text{m}$ -thick sections were rinsed in PBS, incubated with blocking solution (10% donkey normal serum, 0.3% Triton X-100 in PBS) for 1 h at room temperature and stained with primary antibodies in blocking solution at room temperature in a humidified chamber overnight. The following primary antibodies were used: H3K9me2 (Abcam ab1220, 1:500), PCM1 (Santa Cruz [H-262] sc67204, 1:200). Blocking solution was added to negative controls. After washing in PBS, the sections were incubated with the corresponding species-specific fluorophore-conjugated (Cy3 from Jackson, Alexa Fluor® 488 from Molecular Probes) secondary antibodies (1:500) in blocking solution for 1 h at room temperature. The slides were rinsed in PBS, postfixed in 4% paraformaldehyde, washed and mounted with ProLong Gold Antifade Reagent with DAPI (Life Technologies). Immunostained sections were imaged with a Zeiss LSM 700 confocal microscope.

Image stacks were analysed with Volocity Image analysis software (version 6.2.1, Perkin Elmer). Cardiac myocyte nuclei were identified by PCM1- or Nesprin-positive labelling, and analysed for H3K9me2, H3K27me3, GLP and G9a content.

#### **WESTERN AND IMMUNOBLOTTING**

Cells were washed with PBS on ice and then detached from the dish by scraping into PBS. Cells were collected by centrifugation at 1000  $\times$ g for 5 min after which cell pellets were either immediately processed for immunoblotting or snap frozen in liquid N<sub>2</sub>. Cells were solubilised in a modified RIPA buffer containing 150 mM NaCl, 20 mM Tris-HCl, pH 7.4, 10 mM EDTA, 1 mM DTT, 1% each of sodium deoxycholate and TRITON X-100 and 0.1 % SDS. The buffer was supplemented with protease and phosphatase inhibitor cocktails (Sigma Aldrich) and with 0.25 U/ $\mu\text{l}$  of Benzonase (Novagen) to solubilise DNA. After 30 min incubation on ice, the pellet was disrupted by pipetting and after a further 30 min, bath-sonicated for 5 min. Cell debris was subsequently removed by centrifugation at 10,000  $\times$  g for 10 mins at 4°C. Protein concentration of the lysate was determined by the BCA assay (Thermo). 50  $\mu\text{g}$  of protein was resolved by SDS-PAGE on NuPage 4-12% Bis-Tris gradient gels (Life Technologies). Resolved proteins were electrophoretically transferred to 0.1  $\mu\text{m}$  pore size nitrocellulose (histone proteins) or 0.45  $\mu\text{m}$  low fluorescence PVDF (Ehmts; Millipore). Following transfer, non specific protein binding sites were blocked by incubation for 1 h at room temperature in 0.5 $\times$  Odyssey blocking buffer (Licor) diluted in TBS. Primary antibodies were diluted in 0.5 X Odyssey blocking buffer/TBS and incubated overnight at 4°C. The following primary antibodies and dilutions were used: Histone 3 mAb (Sigma Aldrich #H0164; 1:10,000), Calnexin pAb, (Sigma Aldrich #C4731; 1:5000), GAPDH mAb (Sigma Aldrich, #G8795; 1:5000), EHMT2/G9a Rabbit mAb (Abcam #ab133482; 1:1000), EHMT1/GLP mAb (Abcam #ab41969; 1:1000), H3K9me2 mAb (Abcam #ab1220; 1:1000), PCM-1 pAb (Sigma Aldrich, Atlas Prestige antibodies, #HPA023374; 1:1000). Excess antibodies were removed by exchange with 5 washes of TBST over a period of 1 h after which membranes were incubated for 1 hr in TBST containing secondary antibodies conjugated with either Alexa680 (Life Technologies) or IRDye 800 (Licor) diluted at 1:20,000. Secondary antibodies were removed by washing in TBST over a period of 1 hr after which immunoreactive bands were detected using an Odyssey CLx Infrared Imaging System (LI-COR Biosciences). Bands were analysed using Image Studio software (Licor) by creating a boundary around individual bands for quantitation, performing background subtraction as determined for each lane individually and calculating the signal/area within the boundary for each band. The signal/area of bands for the protein of interest to be

quantified was divided by the signal/area of the housekeeping protein in the same lane. Where multiple housekeeping proteins were used for normalization, the above calculations were performed for each individually and then the arithmetic mean for normalized signal/area for proteins of interest presented.

#### ***DATA REPRESENTATION AND STATISTICAL ANALYSIS***

Data are presented as mean  $\pm$  s.e.m. Boxplots and scatter plots display at least 99.5% of data points. At least 3 independent experiments were performed, and unless mentioned otherwise, statistical differences were calculated using a homoscedastic two-tailed Student's *t*-test when comparing 2 conditions, and ANOVA and post-hoc Tukey HSD when comparing more than 2 conditions. Nested ANOVA was applied to immunofluorescence datasets where multiple measurements per sample were available. Changes were accepted to be significant when the *P*-value was below 0.05.

#### ***SUPPLEMENTARY EXPERIMENTAL PROCEDURE REFERENCES***

Alexa, A., and Rahnenfuhrer, J. (2010). topGO: enrichment analysis for gene ontology. R package version 2120.

Andersson, K.B., Birkeland, J.A., Finsen, A.V., Louch, W.E., Sjaastad, I., Wang, Y., Chen, J., Molkenkin, J.D., Chien, K.R., Sejersted, O.M., *et al.* (2009). Moderate heart dysfunction in mice with inducible cardiomyocyte-specific excision of the *Serca2* gene. *Journal of molecular and cellular cardiology* *47*, 180-187.

Benjamini, Y., and Hochberg, Y. (1995). Controlling the false discovery rate: a practical and powerful approach to multiple testing. *Journal of the Royal Statistical Society Series B (Methodological)*, 289-300.

Bergmann, O., Bhardwaj, R.D., Bernard, S., Zdunek, S., Barnabe-Heider, F., Walsh, S., Zupicich, J., Alkass, K., Buchholz, B.A., Druid, H., *et al.* (2009). Evidence for cardiomyocyte renewal in humans. *Science* *324*, 98-102.

Bergmann, O., Zdunek, S., Alkass, K., Druid, H., Bernard, S., and Frisen, J. (2011). Identification of cardiomyocyte nuclei and assessment of ploidy for the analysis of cell turnover. *Experimental cell research* *317*, 188-194.

Bergmann, O., Zdunek, S., Felker, A., Salehpour, M., Alkass, K., Bernard, S., Sjöström, S.L., Szczykowska, M., Jackowska, T., Dos Remedios, C., *et al.* (2015). Dynamics of Cell Generation and Turnover in the Human Heart. *Cell* *161*, 1566-1575.

Boulias, K., and Talianidis, I. (2004). Functional role of G9a-induced histone methylation in small heterodimer partner-mediated transcriptional repression. *Nucleic acids research* *32*, 6096-6103.

Core, L.J., Waterfall, J.J., and Lis, J.T. (2008). Nascent RNA sequencing reveals widespread pausing and divergent initiation at human promoters. *Science* *322*, 1845-1848.

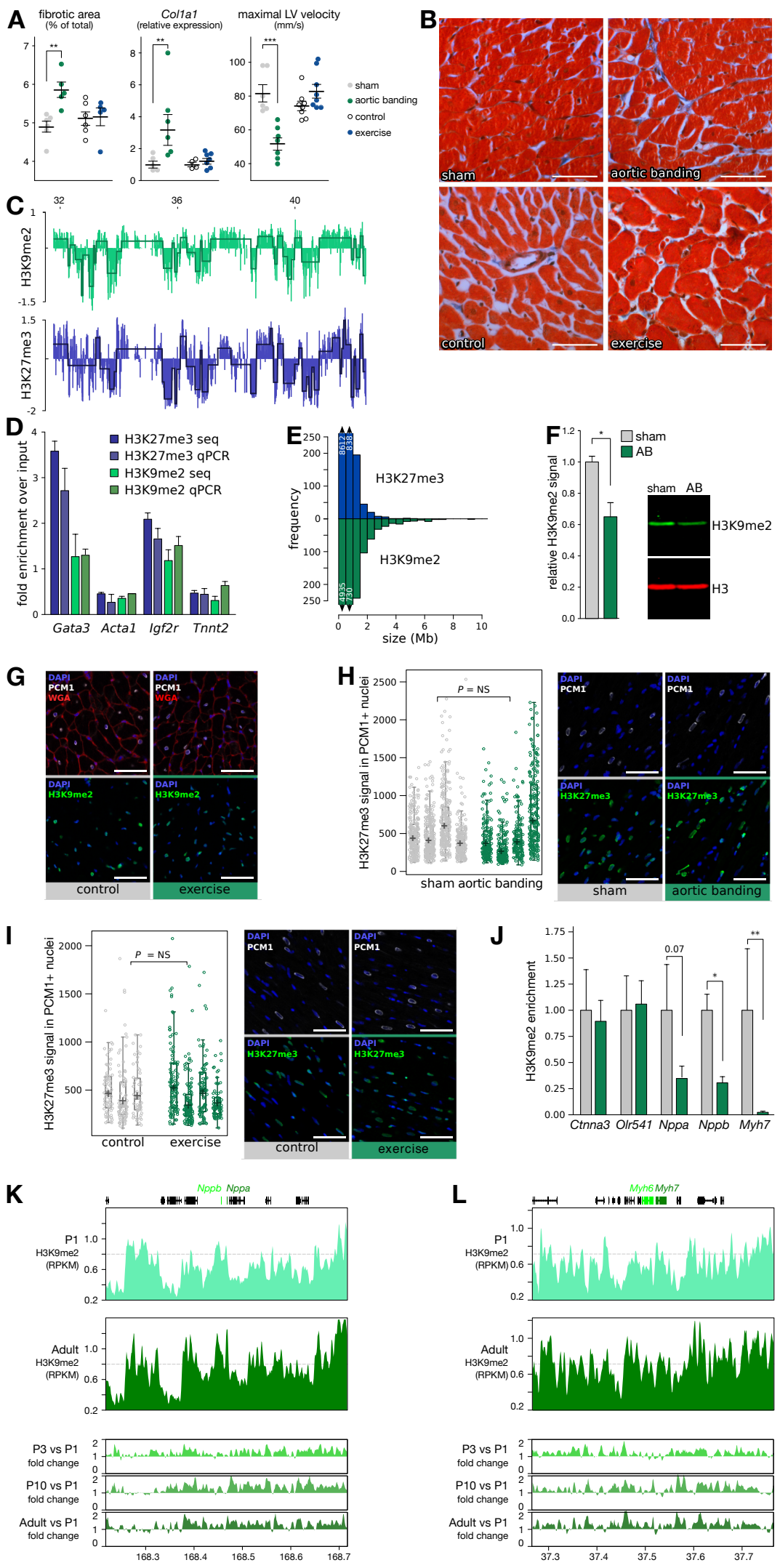
Drawnel, F.M., Wachten, D., Molkenkin, J.D., Maillet, M., Aronsen, J.M., Swift, F., Sjaastad, I., Liu, N., Catalucci, D., Mikoshiba, K., *et al.* (2012). Mutual antagonism between IP(3)RII and miRNA-133a regulates calcium signals and cardiac hypertrophy. *The Journal of cell biology* *199*, 783-798.

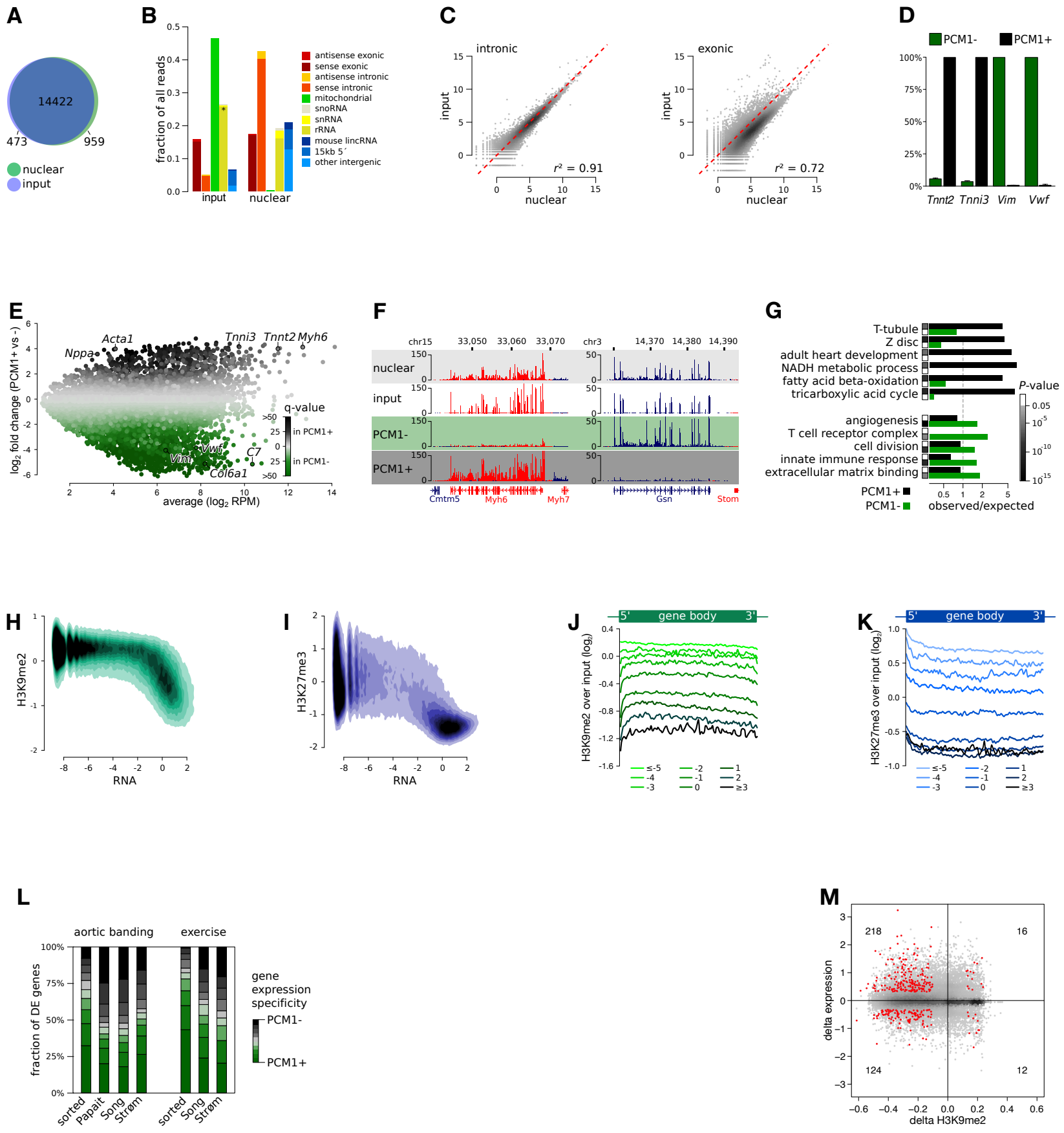
Hahne, F., LeMeur, N., Brinkman, R.R., Ellis, B., Haaland, P., Sarkar, D., Spidlen, J., Strain, E., and Gentleman, R. (2009). flowCore: a Bioconductor package for high throughput flow cytometry. *BMC bioinformatics* *10*, 106.

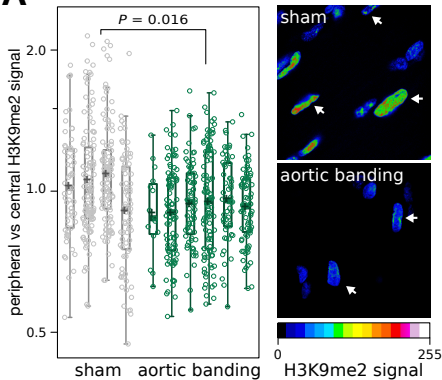
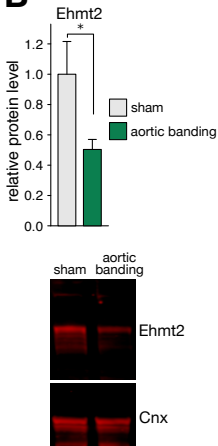
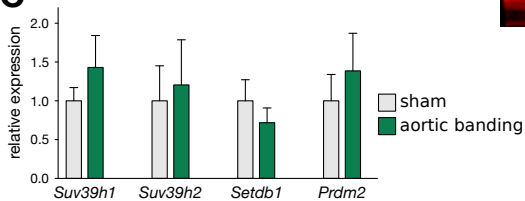
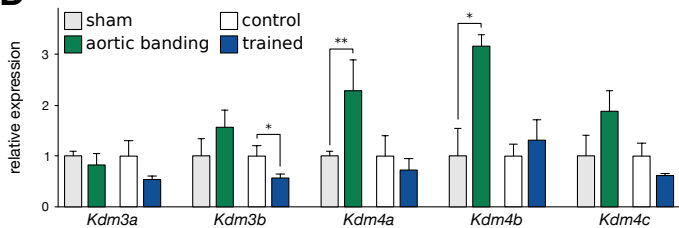
Higazi, D.R., Fearnley, C.J., Drawnel, F.M., Talasila, A., Corps, E.M., Ritter, O., McDonald, F., Mikoshiba, K., Bootman, M.D., and Roderick, H.L. (2009). Endothelin-1-stimulated InsP3-induced Ca<sup>2+</sup> release is a nexus for hypertrophic signaling in cardiac myocytes. *Molecular cell* *33*, 472-482.

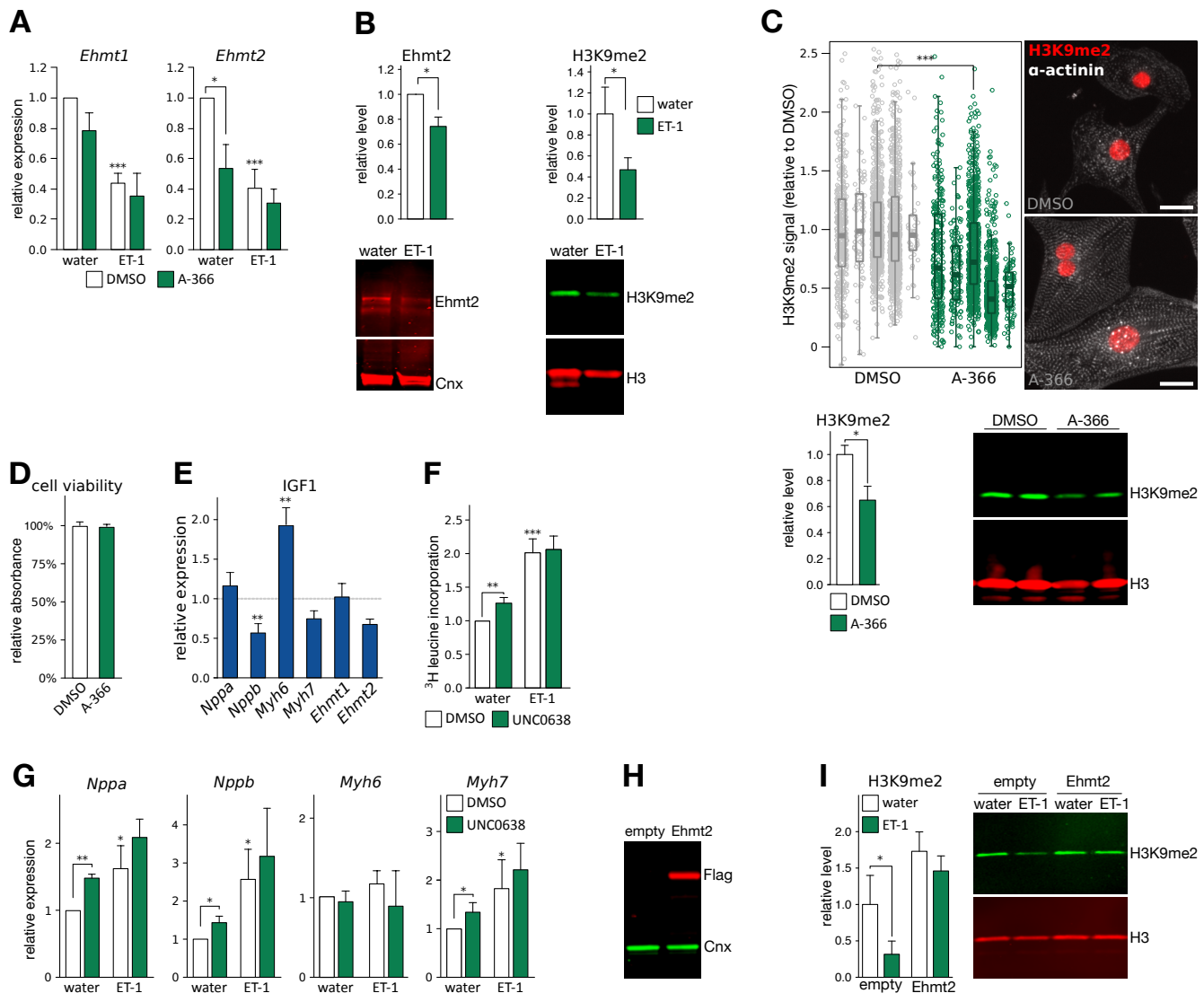
Hougen, K., Aronsen, J.M., Stokke, M.K., Enger, U., Nygard, S., Andersson, K.B., Christensen, G., Sejersted, O.M., and Sjaastad, I. (2010). Cre-loxP DNA recombination is possible with only minimal unspecific transcriptional changes and without cardiomyopathy in Tg(alphaMHC-MerCreMer) mice. *American journal of physiology Heart and circulatory physiology* *299*, H1671-1678.

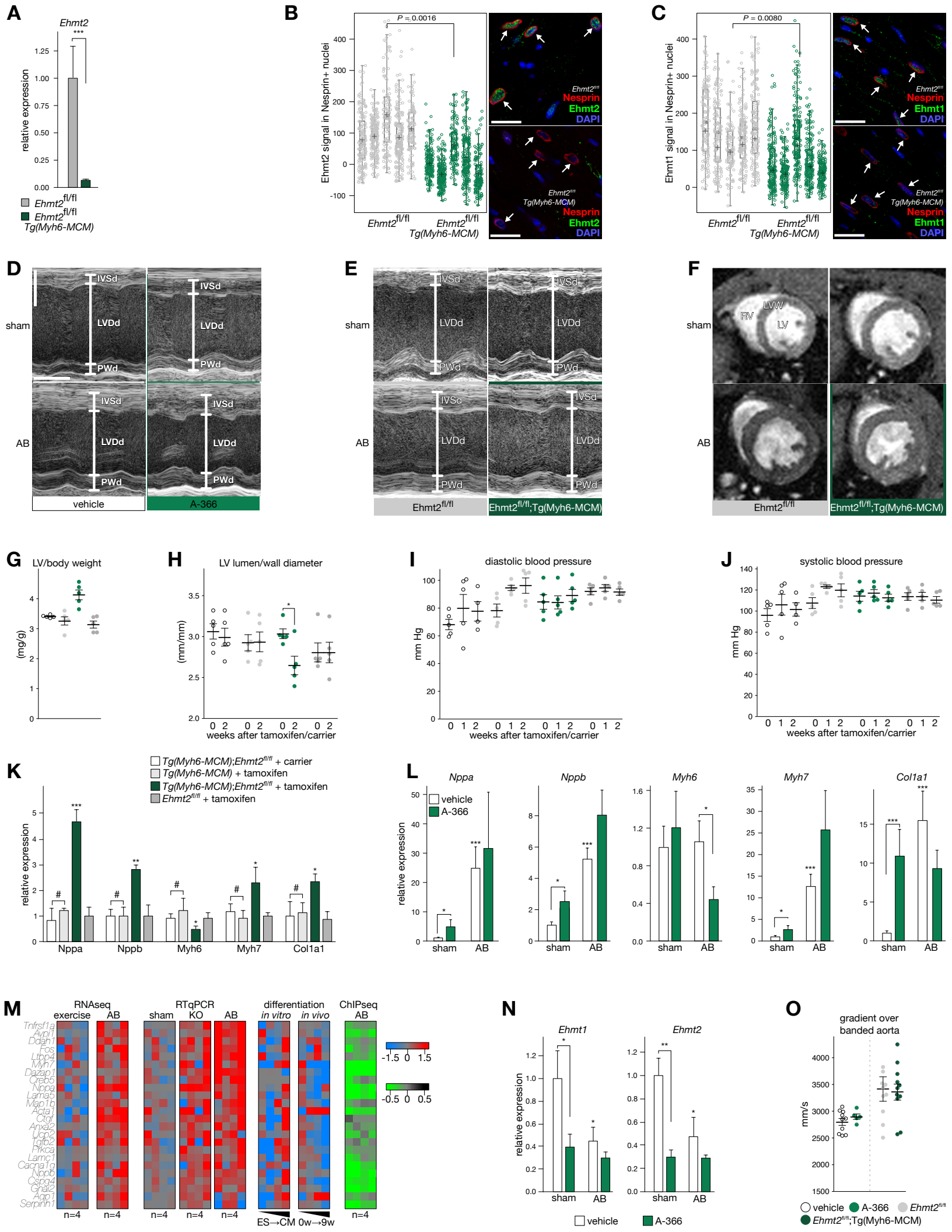
- Langmead, B., Trapnell, C., Pop, M., and Salzberg, S.L. (2009). Ultrafast and memory-efficient alignment of short DNA sequences to the human genome. *Genome biology* *10*, R25.
- Li, H., Handsaker, B., Wysoker, A., Fennell, T., Ruan, J., Homer, N., Marth, G., Abecasis, G., Durbin, R., and Genome Project Data Processing, S. (2009). The Sequence Alignment/Map format and SAMtools. *Bioinformatics* *25*, 2078-2079.
- O'Meara, C.C., Wamstad, J.A., Gladstone, R.A., Fomovsky, G.M., Butty, V.L., Shrikumar, A., Gannon, J.B., Boyer, L.A., and Lee, R.T. (2015). Transcriptional reversion of cardiac myocyte fate during mammalian cardiac regeneration. *Circulation research* *116*, 804-815.
- Papait, R., Cattaneo, P., Kunderfranco, P., Greco, C., Carullo, P., Guffanti, A., Vigano, V., Stirparo, G.G., Latronico, M.V., Hasenfuss, G., *et al.* (2013). Genome-wide analysis of histone marks identifying an epigenetic signature of promoters and enhancers underlying cardiac hypertrophy. *Proceedings of the National Academy of Sciences of the United States of America* *110*, 20164-20169.
- Preker, P., Nielsen, J., Kammler, S., Lykke-Andersen, S., Christensen, M.S., Mapendano, C.K., Schierup, M.H., and Jensen, T.H. (2008). RNA exosome depletion reveals transcription upstream of active human promoters. *Science* *322*, 1851-1854.
- Schindelin, J., Arganda-Carreras, I., Frise, E., Kaynig, V., Longair, M., Pietzsch, T., Preibisch, S., Rueden, C., Saalfeld, S., Schmid, B., *et al.* (2012). Fiji: an open-source platform for biological-image analysis. *Nature methods* *9*, 676-682.
- Sohal, D.S., Nghiem, M., Crackower, M.A., Witt, S.A., Kimball, T.R., Tymitz, K.M., Penninger, J.M., and Molkenstin, J.D. (2001). Temporally regulated and tissue-specific gene manipulations in the adult and embryonic heart using a tamoxifen-inducible Cre protein. *Circulation research* *89*, 20-25.
- Song, H.K., Hong, S.E., Kim, T., and Kim do, H. (2012). Deep RNA sequencing reveals novel cardiac transcriptomic signatures for physiological and pathological hypertrophy. *PloS one* *7*, e35552.
- Strom, C.C., Aplin, M., Ploug, T., Christoffersen, T.E., Langfort, J., Viese, M., Galbo, H., Haunso, S., and Sheikh, S.P. (2005). Expression profiling reveals differences in metabolic gene expression between exercise-induced cardiac effects and maladaptive cardiac hypertrophy. *The FEBS journal* *272*, 2684-2695.
- Strom, C.C., Kruhoffer, M., Knudsen, S., Stensgaard-Hansen, F., Jonassen, T.E., Orntoft, T.F., Haunso, S., and Sheikh, S.P. (2004). Identification of a core set of genes that signifies pathways underlying cardiac hypertrophy. *Comparative and functional genomics* *5*, 459-470.
- Tachibana, M., Nozaki, M., Takeda, N., and Shinkai, Y. (2007). Functional dynamics of H3K9 methylation during meiotic prophase progression. *The EMBO journal* *26*, 3346-3359.
- Team, R.C. (2012). R: A Language and Environment for Statistical Computing. R Foundation for Statistical Computing, Vienna, Austria, 2012 (ISBN 3-900051-07-0).
- Vandesompele, J., De Preter, K., Pattyn, F., Poppe, B., Van Roy, N., De Paepe, A., and Speleman, F. (2002). Accurate normalization of real-time quantitative RT-PCR data by geometric averaging of multiple internal control genes. *Genome biology* *3*, RESEARCH0034.
- Venkatraman, E.S., and Olshen, A.B. (2007). A faster circular binary segmentation algorithm for the analysis of array CGH data. *Bioinformatics* *23*, 657-663.
- Wamstad, J.A., Alexander, J.M., Truty, R.M., Shrikumar, A., Li, F., Eilertson, K.E., Ding, H., Wylie, J.N., Pico, A.R., Capra, J.A., *et al.* (2012). Dynamic and coordinated epigenetic regulation of developmental transitions in the cardiac lineage. *Cell* *151*, 206-220.

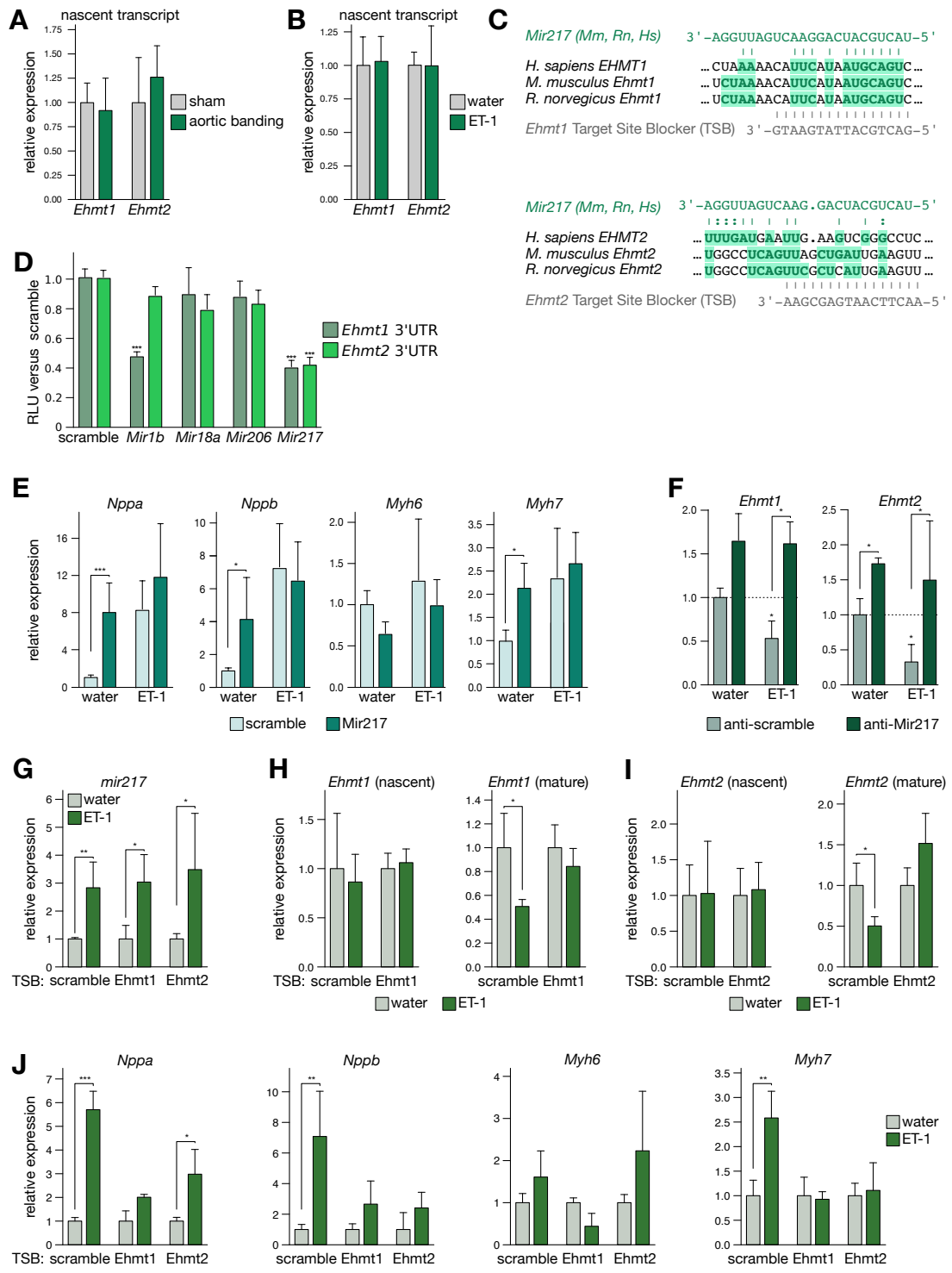


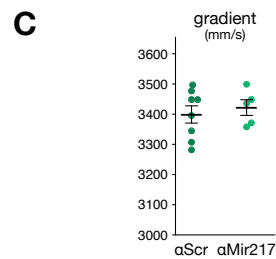
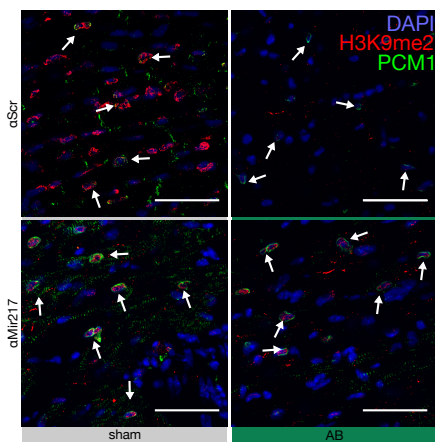
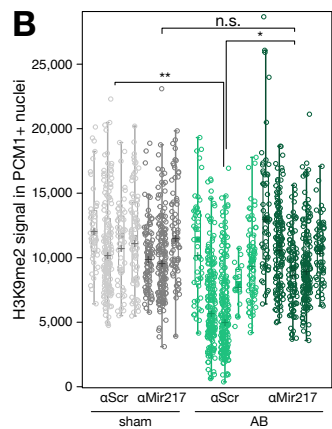
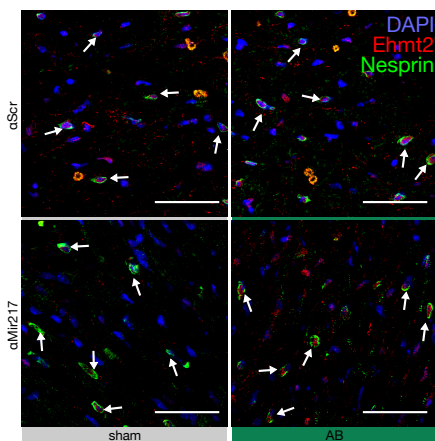
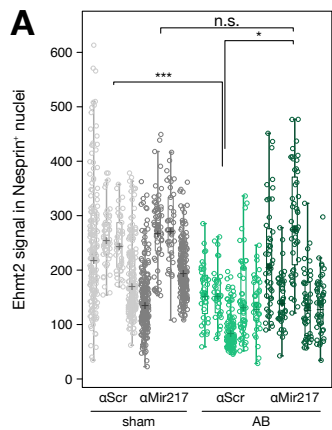


**A****B****C****D**



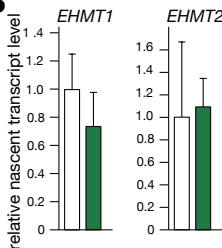
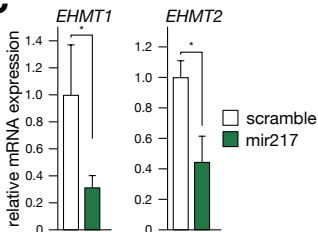






**A**

cardiac examination	age [y]	BMI	cause of death
normal	31	22	suicide
normal	39	34	intoxication
normal	57	22	suicide
normal	57	22	accident
normal	60	24	intoxication
left ventricular hypertrophy	37	20	natural
left ventricular hypertrophy	43	32	natural
cardiomyopathy	57	31	intoxication
left ventricular hypertrophy	61	29	natural
left ventricular hypertrophy	63	30	intoxication

**B****C****D**